J Neurooncol (2011) 101:25–32
DOI 10.1007/s11060-010-0222-9

LABORATORY INVESTIGATION - HUMAN/ANIMAL TISSUE

Morphologic magnetic resonance imaging features of therapy-induced cerebral necrosis

L. R. Rogers · J. Gutierrez · L. Scarpace · L. Schultz · S. Ryu · B. Lord · B. Movsas · J. Honsowetz · R. Jain

Received: 21 September 2009 / Accepted: 4 May 2010 / Published online: 20 May 2010

Abstract To describe the morphologic magnetic resonance imaging (MRI) findings in histologically proven therapy-induced cerebral necrosis. We retrospectively reviewed the morphologic MRI findings in patients with therapy-induced cerebral necrosis. Images were reviewed for size, location, and characteristics of signal intensity abnormalities and T1-contrast enhancement. Images were also assessed for mass effect, necrosis, cyst, atrophy, cortical thinning, and leukoencephalopathy. The individual imaging characteristics were correlated with clinical and treatment variables. There were 44 patients. Seventy percent had a glioma, all patients had received radiation, and 57% had received chemotherapy in close proximity to radiation. All images demonstrated contrast enhancement, predominantly in the white matter. Enhancement was present in the periventricular/subependymal region in 50% of cases and the corpus callosum in 27%. The most common pattern of lesion peripheral enhancement was "spreading wavefront" and of interior enhancement was "Swiss cheese/soap bubble." The enhancing lesion was single in 60% of cases. Mass effect was present in 93% of patients. Location and patterns of enhancement were significantly associated with the interval from brain radiation to the diagnosis of therapy-induced cerebral necrosis, tumor histology, patient age, type of radiation, and administration of systemic chemotherapy. This is the largest study of the morphologic conventional MRI findings in pathologically confirmed therapy-induced cerebral necrosis. We characterized the imaging findings in a variety of tumor types following a variety of radiation treatments and other antineoplastic therapy. These findings may be of value in identifying therapy-induced cerebral necrosis in patients treated for a brain tumor.

Keywords Radiation necrosis · Magnetic resonance imaging · Brain neoplasm · Stereotactic radiosurgery · External beam radiation therapy

L. R. Rogers
Department of Neurology, Henry Ford Hospital, Detroit, MI, USA

L. R. Rogers · L. Scarpace · J. Honsowetz
Department of Neurosurgery, Henry Ford Hospital, Detroit, MI, USA

J. Gutierrez
Department of Pathology, Henry Ford Hospital, Detroit, MI, USA

L. Schultz
Department of Biostatistics and Research Epidemiology, Henry Ford Hospital, Detroit, MI, USA

S. Ryu · B. Lord · B. Movsas
Radiation Oncology, Henry Ford Hospital, Detroit, MI, USA

R. Jain
Diagnostic Radiology, Henry Ford Hospital, Detroit, MI, USA

L. R. Rogers (✉)
Neuro-oncology Program, Neurological Institute, University Hospitals Case Medical Center, 11100 Euclid Avenue, Hanna House Room 506, Cleveland, OH 44106, USA
e-mail: Lisa.Rogers1@UHhospitals.org

Introduction

Therapy-induced cerebral necrosis (TCN) is a consequence of brain radiation, with or without chemotherapy, that is administered for central nervous system (CNS) or extra-CNS neoplasms. It is frequently symptomatic because of progressive enlargement of regions of tissue damage. Therapy-induced cerebral necrosis may require resection, steroids, or

other treatments designed to remove or lessen the necrotic process. Of considerable practical relevance is the distinction of TCN from recurrent/progressive cerebral tumor in patients treated for a brain tumor to avoid unnecessary antineoplastic treatment if TCN is the predominant pathology and to treat for recurrent/progressive tumor if that exists.

The diagnosis of TCN is best established from tissue obtained at surgical resection. A noninvasive method of diagnosis, however, is desirable in order to avoid surgery and is especially relevant for lesions not surgically accessible. To date, no noninvasive imaging modality, including advanced imaging techniques such as perfusion- and diffusion-weighted magnetic resonance (MR) imaging, magnetic resonance spectroscopy (MRS), positron emission tomography (PET), or single photon emission computerized tomography (SPECT), has proven to have adequate sensitivity and specificity to distinguish TCN from recurrent/progressive tumor.

We reviewed the MR imaging of 44 patients with histologically proven TCN to characterize the morphologic features that may be of benefit when evaluating patients in whom TCN or recurrent/progressive tumor are possible.

Materials and methods

Cases were identified by reviewing neuropathology records of all cases of brain surgery that revealed TCN between January 1998 and September 2005. Therapy-induced cerebral necrosis was defined as coagulative necrosis accompanied by treatment-related vascular abnormalities, including vessel wall thickening, necrosis, and hyalinization and endothelial proliferation. To be eligible, the TCN specimen must have been obtained by surgical resection or multiple biopsies and show TCN without visible tumor (pure TCN) or TCN with only isolated microscopic foci of tumor. Patients in whom TCN was mixed with solid viable tumor were excluded. All cases in which the degree of tumor cell infiltration was questionable were re-reviewed by the study neuropathologist (JG).

Living patients consented to an Institutional Review Board-approved protocol that allowed for review of clinical, imaging, and pathology findings. MRIs were reviewed by the study neuroradiologist (RJ). The scan performed immediately before biopsy or resection of TCN was reviewed. Magnetic resonance imaging was performed with 1.5 or 3T scanners. The 1.5T MRI acquisitions included axial FSE T2 images (TR 3500, TE 88, slice thickness 3.0 mm, skip 0.0 mm) and axial T1 pre- and post-contrast images (TR 500, TE 14, slice thickness 3.0 mm, skip 0.0 mm). The 3T MRIs were collected using an eight-channel head coil and included axial T2 FR-FSE (TR 3000, TE 102, slice thickness 5.0 mm, skip 0.0 mm), axial T1 FLAIR pre-contrast (TR 3432, TE 7, flip angle 90, slice thickness 5.0 mm, skip 0.0 mm), and axial T1 FLAIR post-contrast (TR 3431, TE7, flip angle 90, slice thickness 2.5 mm, skip 0.0 mm). Magnetic resonance images were reviewed for the size (product of maximal cross-sectional diameters of the largest lesion), location, and characteristics of signal intensity abnormalities identified on unenhanced T1- and T2-weighted sequences and size, location, and characteristics of T1-contrast enhancement following contrast injection. The interior region of enhancement was defined as "Swiss cheese/soap bubble" when the predominant pattern was multiple small- or moderate-sized areas of enhancement intermixed with foci of necrosis (Fig. 1) in contrast to solid enhancement (Fig. 2). The enhancement margin was defined as "spreading wavefront" when it was predominantly ill-defined and feathery (Figs. 1, 2), not well-demarcated and nodular. Enhancement was classified as focal when there was a single area of enhancement. Multiple sites of enhancement were defined as multicentric if they were within 2 cm of the enhancing margin of the primary TCN lesion or multifocal if they were more than 2 cm from primary TCN lesion (Fig. 3). When

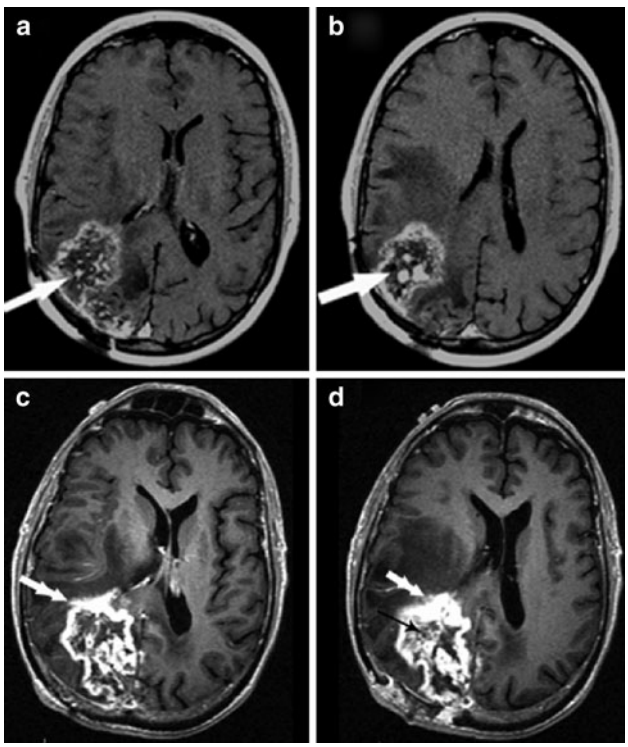

Fig. 1 a–b T1-enhanced MRI in right parietal therapy-induced cerebral necrosis (TCN) shows "Swiss cheese/soap bubble" pattern of internal enhancement (*arrows*). There is also mass effect. **c–d** T1-enhanced MRI in another patient with right parieto-occipital TCN shows the "spreading wavefront" pattern of peripheral enhancement (*double arrows*) and the internal pattern of "Swiss cheese/soap bubble" enhancement (*black arrow*). There is also mass effect anteriorly and laterally. The FLAIR image showed cortical atrophy in the occipital lobe in the region of the observed enhancement

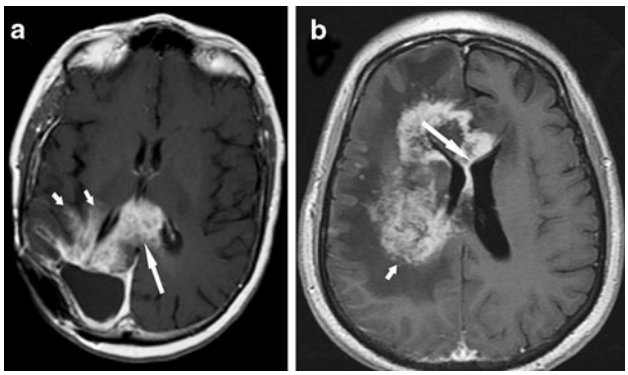

Fig. 2 **a** T1-enhanced MRI in TCN shows a right parietal "spreading wavefront" margin of enhancement (*short arrows*). There is solid internal enhancement. Enhancement is also present in the splenium of the corpus callosum (*long arrow*). **b** The "spreading wavefront" peripheral enhancement pattern (*short arrow*) is present in another patient with TCN. The MRI also demonstrates enhancement in the corpus callosum and periventricular/subependymal regions (*long arrow*)

available, the location of enhancement was correlated with radiation isodose surfaces. Additional findings of mass effect, hemorrhage, necrosis, cyst, atrophy, cortical thinning, and leukoencephalopathy were also assessed. Leukoencephalopathy was graded according to the National Cancer Institute Common Toxicity Criteria, version 3.0.

Statistical methods

We correlated individual imaging characteristics with these demographic, clinical, and treatment variables: age at surgery for TCN, tumor type (primary versus metastatic), type of radiation therapy, administration of chemotherapy or other systemic antineoplastics within 8 weeks of radiation, placement of carmustine wafers, and interval from the first and last date of radiation to the diagnosis of TCN. Although the interval from radiation to TCN varied among patients because of a variety of radiation modalities and duration of treatments, we determined the interval from the first and last day of radiation treatment in order to characterize imaging findings that may present early or delayed after radiation. These correlations among the imaging characteristics and the demographic, clinical, and treatment information were assessed using chi-square tests for the categorical variables of tumor type and specific treatments. Two sample t-tests or analyses of variance methods were conducted to assess the relationships for the continuous variables of age and time. Comparisons were not done when sample size for one of the groups was two or less. P-values less than 0.05 were considered statistically significant. All statistical analyses were performed using SAS 9.1.

Results

Fifty-two patients met the criteria for study. Eight were excluded because MRIs were not available for review or there was inadequate clinical information. The study population included 24 men and 20 women. Median age at the diagnosis of TCN was 49.6 years (range 26–85 years). All patients were treated with brain radiation. All patients had a brain tumor except one radiated for head and neck cancer. The types of tumors and tumor treatments are listed in Table 1. The location of the brain tumor was supratentorial in 41 patients, most commonly in the frontal lobe, solely (15) or involving the adjacent parietal (2) or temporal lobes (1). In one case, a bifrontal glioma was present. The temporal lobe alone was the site of tumor in 10, the parietal lobe in 10, and the occipital lobe in two patients. One

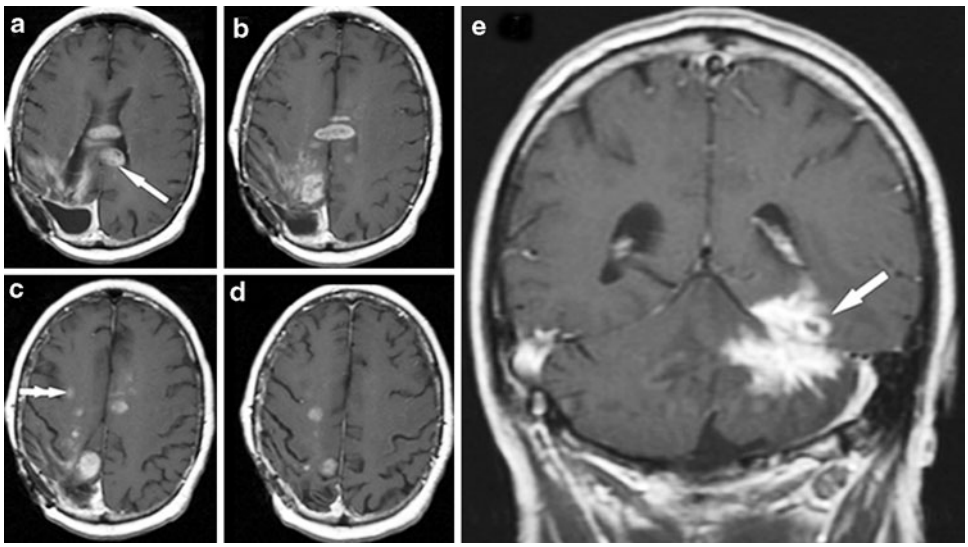

Fig. 3 **a–d** T1-enhanced MRI demonstrates multicentric (<2 cm *long arrow*) and multifocal (>2 cm *double arrow*) enhancement in TCN following treatment for glioblastoma. **e** T1-enhanced coronal MRI in a patient with a left cerebellar metastasis demonstrates multicentric enhancement in the left occipital lobe (*arrow*), adjacent to an enhancing lesion that developed following stereotactic radiosurgery. The occipital lobe lesion was pure TCN at biopsy. Of note, the intervening tentorium is not thickened

Table 1 Clinical and treatment variables and morphologic MR imaging characteristics

Clinical and treatment variables	Number	Percent
Pathology of brain tumor		
High-grade glioma	26	59
Glioblastoma	18	
Anaplastic glioma	8	
Metastasis (Lung 6, breast 2, renal cell 1)	9	20
Low-grade glioma	8	20
Astrocytoma	5	
Oligodendroglioma	2	
Ependymoma	1	
PNET (supratentorial)	1	2
Type of brain tumor surgery		
Subtotal resection	25	57
Gross total resection	14	32
Biopsy	4	9
Type of radiation		
EBRT only	17	39
EBRT + SRS	11	25
SRS only	7	16
EBRT + brachytherapy	7	16
Brachytherapy only	2	5
Systemic chemotherapy within 2 months of RT	25	57
Carmustine wafers	6	14
Imaging characteristics	**Number**	**Percent**
Cortex/white matter enhancement		
Cortex enhancement	27	61
Cortex only	1	2
White matter enhancement	43	98
White matter only	17	39
Cortex and white matter	26	59
Periventricular and/or subependymal enhancement		
Periventricular and subependymal	22	50
Periventricular only	12	27
Subependymal only	1	2
Corpus callosum enhancement	12	27
Pattern of peripheral enhancement		
Spreading wavefront	43	98
Nodular	5	2
Pattern of interior enhancement		
Swiss cheese/soap bubble	40	90
Solid	4	10
Multiplicity of enhancing lesions		
Single lesion	27	61
Multiple lesions	17	39
Multicentric	13	30
Multifocal	4	9
Mass effect	41	93
Location of mass effect		
Sulci	41	93
Ventricle	29	66
Sulci and ventricle	15	34
Sulci, ventricle, and midline	14	32
Midline	14	32
Sulci only	12	27
T1 hyperintensity within hypointensity	26	59
Central necrosis	39	89
Cyst	33	75
Focal atrophy	29	66
Cortical thinning	5	11
Leukoencephalopathy (grade 1 in 18, grade 2 in 1)	19	43

PNET primitive neuroectodermal tumor, *EBRT* external beam radiation therapy, *RT* radiation treatment, *SRS* stereotactic radiosurgery

patient had a large tumor involving the left temporal, parietal, and occipital lobes. Two patients had a cerebellar metastasis. Three glioma patients who received external beam radiation (EBRT) were re-treated with additional EBRT to the same site for suspected or proven tumor recurrence. Among the 18 patients treated with stereotactic radiosurgery (SRS), three received a second SRS treatment to the same site. One of these received a third SRS treatment to a recurrent lesion adjacent to the original tumor site. Brachytherapy was performed with the GliaSite® balloon system in each patient except for one patient treated with permanent I^{125} seeds. Twenty-five patients received systemic chemotherapy or other systemic antineoplastics in close proximity to at least one course of radiation. Surgery for TCN was performed by subtotal resection (24), gross total resection (14), and multiple biopsies (6). Histopathology was pure TCN in 31 patients.

All patients were receiving steroids when the MRI was performed. The median interval from study MRI to surgical resection of TCN was 48 h. The median area of T2 hyperintensity was 52.9 cm (range 3.84–105.82 cm) and the median area of T1 hypointensity was 46.9 cm (range 4.14–95.2 cm). The area of contrast enhancement ranged from 0.96 to 51.66 cm (median 14.5 cm). Table 1 shows the frequency of MRI abnormalities. In 9 of 41 patients with supratentorial tumors, multicentric or multifocal enhancement was present in the adjacent ipsilateral cerebral hemisphere, with or without contralateral enhancement. In eight others, multicentric or multifocal enhancement was identified only in the contralateral cerebral hemisphere. In five of

these cases, the enhancement extended through the corpus callosum, but in three others, the corpus callosum and dura separating the lobes appeared normal. In each of these three, the adjacent lobar enhancement was within the radiation treatment volume of brachytherapy or EBRT and biopsy/resection of the new contralateral lesion revealed pure TCN. In two others treated with SRS for a cerebellar metastasis, dura separating new multicentric enhancement in either the brainstem or the adjacent cerebral hemisphere appeared normal. The lobar lesion in one of these patients was biopsied and revealed pure TCN (Fig. 3). Table 2 shows the significant associations ($P < 0.05$) between the imaging characteristics and clinical and treatment variables. In addition, trends ($P < 0.10$, >0.05) were identified for the following: cysts and younger patient age (47.6 vs. 55.5 years); central necrosis and a smaller mean time between last date of radiation and TCN diagnosis (12.2 vs. 22.7 months) and treatment with brachytherapy, brachytherapy/EBRT, or EBRT/SRS; atrophy and a smaller mean time between last date of radiation and TCN diagnosis (10.9 vs. 18.2 months); leukoencephalopathy and periventricular enhancement and higher patient mean age (53.5 vs. 46.6 years and 51.3 vs. 43.7 years, respectively); and cortical thinning and SRS (80% vs. 36%).

Table 2 Significant ($P < .05$) associations between MR imaging characteristics and clinical and treatment variables

Characteristic/location	Association
Periventricular enhancement	Shorter interval from last date of RT to TCN diagnosis (mean 9.7 vs. 22.9 months)
	Shorter interval from first date of RT to TCN diagnosis (mean 22.2 vs. 30.2 months)
Corpus callosum enhancement	Tumor histology other than metastatic (28 vs. 0%)
Frontal lobe enhancement	Younger patient age (mean 44.0 vs. 56.2 years)
Parietal lobe enhancement	EBRT (91 vs. 67%)
Swiss cheese/soap bubble pattern	Older patient age (mean 50.6 vs. 39.8 years)
	Treatment without SRS (100 vs. 33%)
Single enhancing lesion	Chemotherapy (74 vs. 0%)
Any mass effect	Treatment without SRS (100 vs. 37%)
	Shorter interval between date of last RT to TCN diagnosis (mean, 12.3 vs. 27.9 months)
Central necrosis	Treatment without SRS (100 vs. 33%)
Cortical thinning	Tumor histology of brain metastasis (60 vs. 15%)
Leukoencephalopathy	Higher percentage of carmustine wafer placement (26 vs. 4%)

EBRT external beam radiation therapy, *RT* radiation treatment, *SRS* stereotactic radiosurgery, *TCN* therapy-induced cerebral necrosis

Discussion

The risk of TCN following therapeutic brain radiation for CNS and extra-CNS neoplasms is well recognized. Development of TCN is related to the method of radiation delivery, total dose, fraction size, treatment volume, patient age, and administration of chemotherapy [1]. Therapy-induced cerebral necrosis can occur after EBRT but is most common after high-dose local radiation, such as SRS or brachytherapy. We defined the condition as therapy-induced necrosis, rather than radiation necrosis, because additional antineoplastic therapies can contribute to radiation tissue injury. This is the largest and most comprehensive review of morphologic MRI findings in TCN. In addition, it is the only study for which eligibility was the histologic evidence of pure TCN or TCN with only microscopic foci of tumor. Because the criterion for imaging review was based solely on histology, we are able to characterize MRI findings of TCN associated with a variety of radiation treatment modalities administered for a variety of tumors. We believe that the MRI findings we report are representative of TCN, rather than recurrent tumor, because the majority of our patients (70%) had pure TCN. In addition, the majority of patients (86%) underwent lesion resection, not biopsy.

Signal intensity abnormalities

The most common location of signal intensity abnormality was the frontal lobe, singly or with adjacent lobes. Without performing a review of all patients undergoing brain radiation at our institution, we cannot determine if the high frequency of frontal lobe TCN is due to a high frequency of frontal tumors or to other factors, such as the unique susceptibility of the frontal lobe to radiation injury as is suggested in animal studies [2]. The predominance of MRI white matter abnormalities can be attributed to the predominance of pathologic changes of TCN in white matter. In a histopathology study of radiation injury separate from tumor in patients with malignant gliomas treated with EBRT and chemotherapy, Mahaley et al. identified the predominant pathology as white matter demyelination, coagulative necrosis, vacuolar change, and edema [3]. In our series, the grey matter also frequently showed signal intensity abnormalities. Chan and colleagues identified FLAIR hyperintensity in the grey matter commonly in the temporal lobes of 34 patients who received radiation for nasopharyngeal carcinoma 2 to 10 years previously and in whom 57 temporal lobes showed MRI abnormalities [4].

These cases are of value in evaluating MRI abnormalities of TCN because there is no pre-existing brain tumor or surgical alteration to obscure the imaging findings.

Within regions of T1 hypointensity, we observed irregular, often linear, regions of higher signal intensity in 59% of cases. Two potential explanations are hemorrhagic products and tissue calcification associated with a mineralizing angiopathy induced by radiation. Suzuki and colleagues reported three children with high signal on T1-weighted MRIs after brain radiation in whom computerized tomography demonstrated calcification [5]. Although generally considered to be a late radiation effect, calcification accompanying cerebral radiation necrosis is described within a few weeks of interstitial radiation in animal models [6].

Location and patterns of enhancement

Enhancement was observed in each patient and was present in the white matter of all patients but one. It was accompanied by cortical enhancement in 59% of cases. Peterson and colleagues also described enhancement of both white and grey matter in each of six glioma patients proven or suspected to have radiation necrosis [7]. We suspect that the enhancement is due to the prominent vascular changes associated with brain radiation injury. In Mahaley's series, tissue studies showed vessel wall thickening and fibrinoid alteration, proliferation, and luminal occlusion [3]. Experimental models suggest that brain microvasculature damage is the primary event in the development of late brain radiation injury [8].

Periventricular/subependymal/corpus callosum enhancement

The high frequency of enhancement in the periventricular/subependymal and corpus callosum regions is of clinical significance, as this pattern of enhancement could easily be misinterpreted as tumor invasion, particularly in high-grade glioma patients. The periventricular/subependymal areas may be vulnerable to the tissue-damaging effects of radiation because of the relatively poor blood supply to this region and the unique cellular vulnerability of this region to radiation. Kumar et al. identified corpus callosum enhancement in a smaller percentage of patients in their retrospective study of the MRIs in malignant glioma patients treated with accelerated radiation therapy and carboplatin, followed by chemotherapy, and in whom new enhancing lesions were biopsied and showed radiation necrosis (20 patients) or predominant radiation necrosis defined as necrosis mixed with <20% recurrent and/or residual tumor (16 patients) [9].

The most common enhancement pattern we identified was a "spreading wavefront" periphery in 98% of patients. This pattern was reported by Mullins and colleagues in a retrospective review of MRI findings in high-grade glioma patients treated with proton beam and photon radiation therapy, with or without chemotherapy, who underwent biopsy of new enhancing lesions that showed either predominant recurrent tumor (15 patients) or predominant radiation necrosis (12 patients) [10]. In this study, the "spreading wavefront" pattern was present in six radiation necrosis cases and three with recurrent tumor. Our patients received a variety of radiation treatments and the high frequency of this imaging finding suggests that the pattern can be associated with any type of radiation treatment. A "Swiss cheese/soap bubble" interior enhancement pattern was present in 91% of our patients. This was first described in the report of radiation necrosis by Kumar and colleagues [9]. We identified this as the predominant pattern of interior enhancement in all of our patients treated with EBRT, including those also treated with brachytherapy, and in patients treated with brachytherapy alone. We did not systematically assess the histopathology of TCN at these sites, and the histopathology of these enhancement patterns, as compared with the less common solid nodular pattern of enhancement, is not known.

Number of enhancing lesions

Multicentric or multifocal enhancing lesions were present in 40% of our cases. Because the radiation dosimetry was not available for many patients, especially those who received part of or all of their radiation treatment elsewhere, we were not able to systematically correlate the location of enhancement with the radiation dose distribution. Kumar and colleagues determined that the enhancing radiation necrosis lesions occurred within the treatment volume [9]. Peterson et al. reported that multifocal areas of contrast enhancement were within the treatment volume but outside the maximum radiation dose [7]. In the majority of our cases of supratentorial TCN, the multicentric or multifocal lesions were in the ipsilateral hemisphere. In eight others, they were in the opposite cerebral hemisphere and, in three of these, adjacent to the intervening falx. In the two patients with cerebellar tumors, multicentric enhancement was observed in the temporal or occipital lobe (two patients) and in the adjacent brainstem (one patient) separated by the tentorium. In each of these five cases, the dura appeared normal, without significant dural thickening or nodularity. In the cases of contralateral hemisphere supratentorial TCN, there was also no corpus callosum imaging abnormality. We documented pure TCN in each of four of these patients who underwent biopsy or resection of the multicentric lesion.

Other imaging findings

We observed mass effect, central necrosis, and cysts in the majority of patients. Local atrophy was present in two-thirds of our cases, but we were unable to distinguish volume loss secondary to radiation from that due to tumor surgical intervention, such that the significance of this finding is uncertain. Five of our patients had focal cortical thinning near the enhancement, but we were similarly unable to distinguish cortical thinning from postsurgical changes, and we may have underestimated it. Chan and colleagues reported thinning of the cortex in 63% of temporal lobes with radiation injury identified on MR who had not undergone brain surgery [4].

Correlation of imaging characteristics with clinical and treatment variables

Correlations of potential clinical significance include a significantly lower frequency of "Swiss cheese/soap bubble" enhancing pattern, central necrosis, and mass effect following SRS (either alone or with EBRT) than other types of radiation. In addition, there was a significant correlation between periventricular enhancement and a shorter time from the initial and last dates of radiation treatment. This temporal pattern of enhancement may be in accordance with the clinical observation that periventricular enhancing lesions seen early after brain radiation may regress. Mass effect correlated with a shorter interval from the last date of radiation, suggesting that treatment-related brain mass effect may regress. Lastly, corpus callosum enhancement was not identified in any patient with TCN following treatment for a brain metastasis.

Limitations

Any imaging study that seeks to define diagnostic features of TCN must be interpreted cautiously because TCN is an evolving dynamic process and the morphologic imaging features may change over time. For example, early imaging enhancement after EBRT or SRS ("pseudoprogression") can stabilize or regress and the pathobiology of this condition may vary from that of delayed TCN [11, 12]. In addition, an incomplete tissue resection in some patients can result in a sampling error within a more extensive area of tumor mixed with TCN. This is a potential limitation of most brain tissue collection studies. The imaging features we describe cannot be considered pathognomonic for TCN, and they do not exclude disease progression. Only a case-matched control series comparing MRI characteristics of patients with recurrent/progressive tumor or with TCN will determine the specificity of our findings to TCN. In addition, we did not compare the morphologic MRI features with advanced imaging techniques sometimes used to differentiate TCN from recurrent tumor. One area for future research is to combine routine and advanced imaging techniques to determine if combined data will be of benefit in distinguishing the histology.

Conclusions

This is the largest study of morphologic MRI findings in pathologically confirmed TCN. Although the number of patients receiving high dose local radiation (brachytherapy or SRS) alone was relatively low, we believe the MRI features we describe can assist in the clinical diagnosis of TCN after any type of radiation for a brain tumor. These findings may be of value in determining appropriate therapeutic intervention for new enhancing lesions that develop after radiation for a brain tumor.

Disclosures The authors report no financial relationships, sponsorships, or affiliations.

References

1. Marks JE, Baglan RJ, Prassad SC, Blank WF (1981) Cerebral radionecrosis: incidence and risk in relation to dose, time, fractionation and volume. Int J Radiat Oncol Biol Phys 7:243–252
2. Calvo W, Hopewell JW, Reinhold HS, Yeung TK (1988) Time- and dose-related changes in the white matter of the rat brain after single doses of X rays. Br J Radiol 61:1043–1052
3. Mahaley MS Jr, Vogel FS, Burger P, Ghatak NR (1977) Neuropathology of tissues from patients treated by the Brain Tumor Study Group. Natl Cancer Inst Monogr 46:7–82
4. Chan YL, Leung SF, King AD, Choi PH, Metreweli C (1999) Late radiation injury to the temporal lobes: morphologic evaluation at MR imaging. Radiology 213:800–807
5. Suzuki S, Nishio S, Takata K, Morioka T, Fukio M (2000) Radiation-induced brain calcification: paradoxical high signal intensity in T1-weighted MR images. Acta Neurochir 142:801–804
6. Mishima N, Tamiya T, Matsumoto K, Furuta T, Ohmoto T (2003) Radiation damage to the normal monkey brain: experimental study induced by interstitial irradiation. Acta Med Okayama 57:123–131
7. Peterson K, Clark HB, Hall WA, Truwit CL (1995) Multifocal enhancing magnetic resonance imaging lesions following cranial irradiation. Ann Neurol 38:237–244
8. Coderre JA, Morris GM, Micca PL, Hopewell JW, Verhagen I, Kleiboer BJ, van der Kogel AJ (2006) Late effects of radiation on the central nervous system: Role of vascular endothelial damage and glial stem cell survival. Radiat Res 166:495–503
9. Kumar AJ, Leeds NE, Fuller GN, Tassel P, Maor MH, Sawaya RE, Levin VA (2000) Malignant gliomas: MR imaging spectrum of radiation therapy- and chemotherapy-induced necrosis of the brain after treatment. Radiology 217:377–384
10. Mullins ME, Barest GD, Schaefer PW, Hochberg FH, Gonzaleza RG, Lev MH (2005) Radiation necrosis versus glioma recurrence:

conventional MR imaging clues to diagnosis. AJNR 26:1967–1972
11. Ross DA, Sandler HM, Balter JM, Hayman JA, Archer PG, Auer DL (2002) Imaging changes after stereotactic radiosurgery of primary and secondary malignant brain tumors. J Neurooncol 56:175–181
12. Taal W, Brandsma D, de Bruin HG, Bromberg J, Swaak-Kragten A, Sillevis Smitt P, Van Es CA, Van Den Bent MJ (2008) Incidence of early pseudo-progression in a cohort of malignant glioma patients treated with chemoirradiation with temozolomide. Cancer 113:405–410